

Finite element based total response analysis of rectangular liquid containers against different excitations

Kalyan Kumar Mandal*

Department of Civil Engineering, Jadavpur University, India

(Received December 2, 2021, Revised March 5, 2023, Accepted March 17, 2023)

Abstract. In the present study, the total hydrodynamic pressure exerted by the fluid on walls of rectangular tanks due to horizontal excitations of different frequencies, is investigated by pressure based finite element method. Fluid within the tanks is inviscid, compressible and its motion is considered to be irrotational and it is simulated by two dimensional eight-node isoparametric. The walls of the tanks are assumed to be rigid. The total hydrodynamic pressure increases with the increase of exciting frequency and has maximum value when the exciting frequency is equal to the fundamental frequency. However, the hydrodynamic pressure has decreasing trend for the frequency greater than the fundamental frequency. Hydrodynamic pressure at the free surface is independent to the height of fluid. However, the pressure at base and mid height of vertical wall depends on height of fluid. At these two locations, the hydrodynamic pressure decreases with the increase of fluid depth. The depth of undisturbed fluid near the base increases with the increase of depth of fluid when it is excited with fundamental frequency of fluid. The sloshing of fluid within the tank increases with the increase of exciting frequency and has maximum value when the exciting frequency is equal to the fundamental frequency of liquid. However, this vertical displacement is quite less when the exciting frequency is greater than the fundamental frequency.

Keywords: compressibility of water; finite element method; fundamental frequency; sloshed displacement; total hydrodynamic pressure

1. Introduction

Tank in rectangular shape is very common to store liquids such as liquid oxygen, nitrogen, and water and petroleum product. These liquid containers may suffer considerable damage if the behaviour during vibration is not predicted properly.

Ming and Duan (2010) carried out the numerical simulation of sloshing in rectangular tank with VOF based on unstructured grids. A mesh free particle approach-based MPS method was used to investigate the sloshing behaviour of a partially filled liquid container by Jena and Biswal (2018). The finite element methods of pseudo-static seismic analysis and response analysis were presented. Bouaanani (2012) used sub-structuring approach where the flexible liquid-containing structure and the impulsive effects of the fluid domain were modeled using finite element and analytically respectively. Three-dimensional (3D) ground-supported cylindrical and rectangular rigid liquid storage tanks filled with water were analysed using coupled acoustic-structural (CAS) and coupled

*Corresponding author, Dr., E-mail: kkma_iitkgp@yahoo.co.in

Eulerian-Lagrangian (CEL) approaches by Rawat *et al.* (2019). It was found that the non-linearity of the sloshing wave displacement did not play a significant role in calculating the hydrodynamic pressure distribution on the rigid tank walls. The free vibration of two-dimensional deformable rectangular tanks filled with a compressible, irrotational and inviscid fluid was analytically investigated by Pajand (2016). Kolai and Rakheja (2018), Kang *et al.* (2019) and Yazdabad *et al.* (2018) studied free vibration of liquid in tank of flexible membrane with the liquid surface constrained using Finite Element Model. Shake table experiments were performed by Sanapala *et al.* (2019) and Sahaj *et al.* (2021) to study the fluid structure interaction effects between the sloshed liquid and the internal structure. Higher hydrodynamic pressures were observed near the liquid free surface compared to those measured near the tank base. Similarly, Kotrasova and Kormanikova (2018) experimentally studied the sloshing of liquid in partially and fully filled ground supported cylindrical container subjected to external excitation horizontal harmonic motion. A review study on liquid storage tanks was carried out by Zhao and Zhou (2018).

Nonlinear numerical simulations were performed for practical tanks under different horizontal and vertical near fault excitations by Hejazi and Mohammadi (2019). A numerical code based on potential flow theory using Boundary Element Method was developed Zhao *et al.* (2018). Shekari *et al.* (2019) numerically analysed the simultaneous influences of base-isolator system and vertical baffle on the seismic performance of a three-dimensional (3D) rectangular liquid storage container. The sloshing behaviour of fluid due to harmonic excitation for different tank lengths was investigated using finite element analysis in Eulerian approach by Mandal and Maity (2016) and Adhikary and Mandal (2018). Chu *et al.* (2018) investigated the sloshing phenomenon in a rectangular water tank with multiple bottom-mounted baffles using laboratory experiments and a Large Eddy Simulation (LES) model. The kinematic motion of water surface was solved by Volume of Fluid (VOF) method. Similarly, smoothed particle hydrodynamics was used to determine the hydrodynamic pressure by Nguyen *et al.* (2021). A numerical code was developed to work out the pressure distribution on the rectangular and trapezoidal storage tanks' perimeters due to liquid sloshing phenomenon using Laplace equation and finite element method by Saghi (2016). The results showed that the free surface fluctuation in the trapezoidal storage tanks arrived to the maximum value in less time in comparison with the rectangular storage tank. Hydrodynamic pressures for rectangular tanks were analysed considering the effect of wall flexibility on impulsive pressures by Chen and Kianoush (2004). Algreane *et al.* (2011) modified the adding of impulsive mass to elevated tank instead to Westergaard approach. Dudhatra and Desani (2016) parametrically studied ground rested rectangular RC tank considering different length to depth ratio. The seismic analysis was performed considering water to be impulsive mass and convective mass suggested by GSDMA guidelines. Yazdanian *et al.* (2016) analysed rectangular water storage concrete tanks using static, modal, and response-spectrum approaches.

Aregawi and Kassahun (2017) investigated an idealized ground supported reinforced concrete rectangular water tank under earthquake excitation using linear three-dimensional finite element analysis and SAP2000 software. Dynamic analysis of elevated water tanks supported on RC framed structure was studied by Ali and Telang (2017) using STAAD Pro V8i SS6 software. Similarly, the impulsive and convective pressure on supporting structure as well as rectangular tank was evaluated by Hemalatha and Rao (2018) using STAAD Pro. Sloshing effect on elevated water tank was studied using Finite Element Method (FEM) based on software ANSYS by Wakchaure and Besekar (2014). Kotrasova (2017) studied ground supported water tank as endlessly long shipping channel under horizontal seismic excitation rested on hard or sub-soil using ADINA software. Mingzhen and Lin (2018) studied ground supported RC water tank under bi-directional horizontal seismic excitation

using ADINA. Bhojavia and Dhyani (2018) analysed soft, medium and hard soil rested circular water tank under seismic excitation with different diameter/height ratio. Total base shear, total base moment, and maximum hydrodynamic pressure were found to be decreased with the increase of d/h ratio. Patel *et al.* (2012) studied sloshing of elevated water tank of different column proportionality under seismic excitation using SAP 2000. Zhaoac *et al.* (2018) reviewed and summarized the response of concrete liquid tank using SAP 2000 based on seismic loads of ACI 350.3. Arafa (2007) investigated the liquid sloshing effect of rectangular tank under horizontal base excitation using finite element formulation with liquid velocity potential as nodal degree of freedom. The effect of three-dimensional geometry on the seismic response of open-top rectangular concrete water tanks was investigated by Avval (2012) considering fluid structure interaction with wall flexibility using ANSYS.

Based on the existing literatures, it is found the total responses of liquid containers depend on external excitations and finite element analysis is identified as an efficient numerical for determine the total responses of liquid containers. Generally, displacement, displacement potential and velocity potential are considered to be nodal variable for finite element modeling. However, the pressure based formulation is advantageous as it satisfies irrotational condition automatically. In the present study, a pressure based finite element model is proposed to determine total responses water within rectangular tanks against different horizontal excitations. The water is considered as compressible and inviscid and its motion is assumed to be irrotational. A computer code in MATLAB environment has been developed to obtain the total responses. The study is carried out for different sizes of tank against horizontal external excitations

2. Theoretical formulation

The total stress tensor, σ_{ij} for Newtonian fluid is defined as

$$\sigma_{ij} = -P\delta_{ij} + \sigma'_{ij} \quad (1)$$

Where, σ'_{ij} depends on deformation rate and is called as viscous stress tensor. P , hydrodynamic pressure is independent on the rate of deformation and Δ_{ij} is kronecker delta. Now, σ'_{ij} for linear elastic media

$$\sigma'_{ij} = \psi\Delta\delta_{ij} + 2\mu D_{ij} \quad (2)$$

Where, μ and ψ are two material constants. μ is viscosity and $(\psi+2\mu/3)$ is bulk viscosity. D_{ij} is deformation tensor. D_{ij} is defined as

$$D_{ij} = \frac{1}{2} \left(\frac{\partial v_i}{\partial y_j} + \frac{\partial v_j}{\partial x_i} \right) D = D_{11} + D_{22} + D_{33} \quad (3)$$

Thus, σ_{ij} becomes

$$\sigma_{ij} = -P\Delta\delta_{ij} + \psi\Delta\delta_{ij} + 2\mu D_{ij} \quad (4)$$

The bulk viscosity, $(\psi+2\mu/3)$, for compressible fluid becomes zero and Eq. (4) reduced to

$$\sigma_{ij} = -P\Delta_{ij} - \frac{2\mu}{3}\Delta\delta_{ij} + 2\mu D_{ij} \quad (5)$$

If we neglect the viscosity of fluid, Eq. (5) becomes

$$\sigma_{ij} = -P\Delta\delta_{ij} \quad (6)$$

Again, the equation of motion or Navier-Stokes are expressed as

$$\rho \left(\frac{\partial v_i}{\partial t} + v_j \frac{\partial v_i}{\partial x_j} \right) = \frac{\partial \sigma_{ij}}{\partial x_j} + \rho B_i \sigma \kappa \quad (7)$$

$$\rho \left(\frac{\partial v_i}{\partial t} + v_j \frac{\partial v_i}{\partial x_j} \right) = \rho B_i - \frac{\partial \rho}{\partial x_i} \quad (8)$$

If we neglect the convective terms in above equations and if f_x and f_y are body forces, u and v are the velocity components along x and y axes respectively eqs. (7) to (8) reduced to

$$\frac{1}{\rho} \frac{\partial P}{\partial x} + \frac{\partial u}{\partial t} = f_x \quad (9)$$

$$\frac{1}{\rho} \frac{\partial P}{\partial y} + \frac{\partial v}{\partial t} = f_y \quad (10)$$

Eqs. (9) and (10) can be expressed bellow if body forces are neglecting

$$\frac{1}{\rho} \frac{\partial P}{\partial x} + \frac{\partial u}{\partial t} = 0 \quad (11)$$

$$\frac{1}{\rho} \frac{\partial P}{\partial y} + \frac{\partial v}{\partial t} = 0 \quad (12)$$

In two dimensions, the continuity equation is defined as

$$\frac{\partial \rho}{\partial t} + \rho \alpha^2 \left(\frac{\partial u}{\partial x} + \frac{\partial v}{\partial y} \right) \quad (13)$$

Where, α expresses acoustic wave speeds in liquid. After, differentiating eqs. (11) to (12), the following expression may be obtained.

$$\frac{1}{\rho} \frac{\partial^2 P}{\partial x^2} + \frac{\partial}{\partial x} \left(\frac{\partial u}{\partial t} \right) = 0 \quad (14)$$

$$\frac{1}{\rho} \frac{\partial^2 P}{\partial y^2} + \frac{\partial}{\partial y} \left(\frac{\partial v}{\partial t} \right) = 0 \quad (15)$$

Adding the above two equations finally we arrived Eq. (16).

$$\frac{1}{\rho} \frac{\partial^2 P}{\partial x^2} + \frac{1}{\rho} \frac{\partial^2 P}{\partial y^2} + \frac{\partial}{\partial x} \left(\frac{\partial u}{\partial t} \right) + \frac{\partial}{\partial y} \left(\frac{\partial v}{\partial t} \right) = 0 \quad (16)$$

Time derivative of Eq. (13) can be expressed as

$$\frac{\partial^2 P}{\partial t^2} + \rho \alpha^2 \left\{ \frac{\partial}{\partial x} \left(\frac{\partial u}{\partial t} \right) + \frac{\partial}{\partial y} \left(\frac{\partial v}{\partial t} \right) \right\} = 0 \quad (17)$$

Now, from eq. (16) to (17) we can get Eq. (18)

$$\frac{1}{\rho} \frac{\partial^2 P}{\partial x^2} + \frac{1}{\rho} \frac{\partial^2 P}{\partial y^2} - \frac{1}{\rho \alpha^2} \frac{\partial^2 P}{\partial t^2} = 0 \quad (18)$$

Thus, the Eq. (18) can be expressed as bellow for compressible fluid and it is known as Helmholtz's equation.

$$\nabla^2 P(x, y, t) = \frac{1}{\alpha^2} \ddot{P}(x, y, t) \quad (19)$$

If we neglect the compressibility of fluid Eq. (19) reduced to Eq. (20). It is known as Laplace's equation

$$\nabla^2 P(x, y, t) = 0 \quad (20)$$

Readers are referred to Adhikary and Mandal (2018) for detail procedure. The hydrodynamic pressure within the liquid may be determined by solving Eq. (19) with some boundary conditions expressed bellow. Fig. 1 shows a typical tank-liquid system.

1) At surface I

The condition at the top surface of liquid is considered as

$$\frac{1}{g} \ddot{P} + \frac{\partial P}{\partial y} = 0 \quad (21)$$

2) At surface II

At liquid-wall interface, the pressure gradient should satisfy

$$\frac{\partial P}{\partial n}(0, y, t) = \rho_f a \quad (22)$$

Where, ρ_f and a are fluid density and horizontal ground acceleration respectively.

3) At surface III

Pressure gradient along this surface should be considered as zero.

$$\frac{\partial P}{\partial n}(x, 0, t) = 0.0 \quad (23)$$

2.1 Finite element formulation

Eq. (19) may be expressed in discretized form as Eq. (24). In this expression, pressure is considered to be the nodal variable.

$$\int_{\Omega} N_{rj} [\nabla^2 \sum N_{ri} P_i - \frac{1}{\alpha^2} \sum N_{ri} \ddot{P}_i] d\Omega = 0 \quad (24)$$

Where, N_{rj} is the shape function for the reservoir domain, Ω .

Applying Green's theorem eq. (24) may be reduced to

$$- \int_{\Omega} \left[\frac{\partial N_{rj}}{\partial x} \sum \frac{\partial N_{ri}}{\partial x} P_i + \frac{\partial N_{rj}}{\partial y} \sum \frac{\partial N_{ri}}{\partial y} P_i \right] d\Omega - \frac{1}{\alpha^2} \int_{\Omega} N_{rj} \sum N_{ri} d\Omega \ddot{P}_i + \int_{\Gamma} N_{rj} \sum \frac{\partial N_{ri}}{\partial n} d\Gamma P_i = 0 \quad (25)$$

where surface of the fluid domain is represented by Ω and boundary of fluid domain is represented by Γ . The last term of Eq. (25) may be expressed as

$$B = \int_{\Gamma} N_{rj} \frac{\partial P}{\partial n} \quad (26)$$

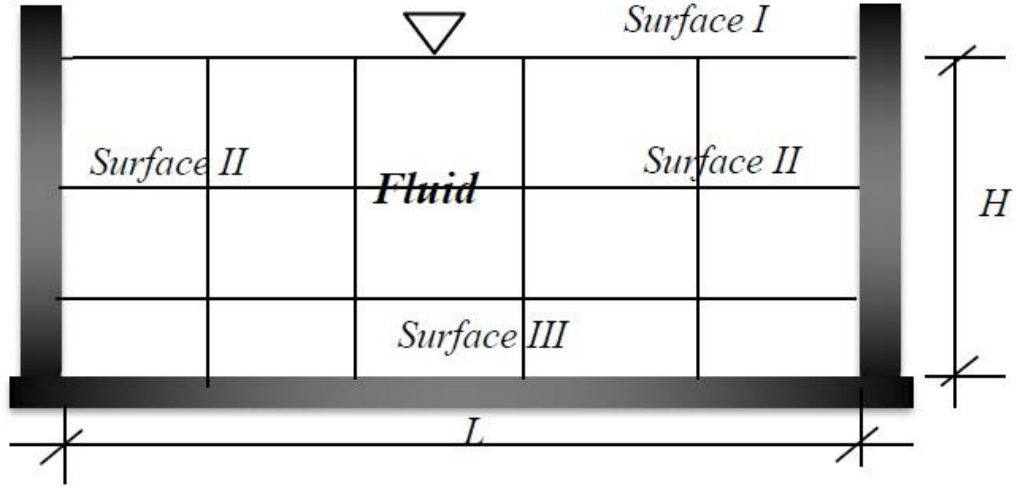


Fig. 1 Geometry and finite element meshing of tank-water system

In matrix form the Eq. (26) may be written as

$$(\overline{EE})\overline{\ddot{P}} + (GG)\overline{P} = \overline{F} \quad (27)$$

In which

$$\overline{EE} = \frac{1}{\alpha^2} \sum \int_{\Omega} N_r^T N_r d\Omega \quad (28)$$

$$GG = \sum \int_{\Omega} \left[\frac{\partial N_r^T}{\partial x} \frac{\partial N_r}{\partial x} + \frac{\partial N_r^T}{\partial y} \frac{\partial N_r}{\partial y} \right] d\Omega \quad (29)$$

$$F = \sum \int_{\Gamma} N_r^T \frac{\partial P}{\partial n} d\Gamma = \overline{F}_I + \overline{F}_{II} + \overline{F}_{III} \quad (30)$$

Here, *I*, *II* and *III* represent different surface boundary. For sloshing at free surface, the Eq. (21) may be expressed as

$$\overline{F}_I = -\frac{1}{g} S_f \overline{\ddot{P}} \quad (31)$$

Where

$$S_f = \sum \int_{\Gamma_f} N_r^T N_r d\Gamma \quad (32)$$

At tank- fluid interface, *II*, $\{a\}$ is the nodal acceleration vector in generalized coordinates, and expressed as

$$F_{II} = -\rho R_{II} \overline{a} \quad (33)$$

In which

$$S_{II} = \sum \int_{\Gamma_{11A}} n d^{1v} N_r^T N_r d\Gamma \quad (34)$$

At tank bottom surface, III

$$\bar{F}_{III} = 0 \quad (35)$$

Readers are referred to Adhikary and Mandal (2018) for detail implementation procedure. After imposing all boundary condition, the Eq. (27) becomes

$$(EE)\bar{P} + (AA)\bar{P} + (GG)\bar{P} = \bar{F}_r \quad (36)$$

Where

$$EE = \bar{E}\bar{E} + \frac{1}{g}S_I \quad (37)$$

$$\bar{F}_r = -\rho_f S_{II}\bar{a} - \rho_f S_{IV}\bar{a} \quad (38)$$

Hydrodynamic pressure is obtained after solving eq. (26) for given acceleration at the tank-fluid interface.

2.2 Computation of velocity and displacement of fluid

After obtaining hydrodynamic pressure, the acceleration of fluid may be calculated from Eq. (11) to (12). Whereas, the velocity at any instant of time is determined from Gill's time integration scheme (Gill 1951) which is a step-by-step integration procedure based on Runge-Kutta method (Ralston and Wilf 1965). Velocity at time equal to t will be expressed as

$$v_t = v_{t-\Delta t} + \Delta t \dot{v}_t \quad (39)$$

Similarly, the displacement, d at time equal to t may be expressed as

$$d_t = d_{t-\Delta t} + \Delta t v_t \quad (40)$$

3. Results and discussions

3.1 Validation of the proposed algorithm.

In this section, a bench marked problem is solved and results are compared with the results obtained by Virella *et al.* (2008) to determine the accuracy of present algorithm. The geometric and material properties of the tank are as follows: height of water in the tank (H) = 6.10 m, length of tank (L) = 30.5 m, so that ratio of height to length (H/L) = 0.2, density of water = 983 kg/m³, pressure wave velocity = 1451 m/s. Here, the fluid is discretized by 4×8 (i.e., $N_h = 4$ and $N_v = 8$). The first three natural time periods of the tank fluid are listed and compared with those values obtained by Virella *et al.* (2008) in Table 1. The tabulated results show the accuracy of the present method.

3.2 Selection of time step

The results from Newmark's integration technique are quite sensitive to the time step and to determine a suitable time step, tank with following properties are considered. Water depth (H) = 1.6

Table 1 First three natural time period of the tank fluid

Mode number	Natural Time period in sec	
	Present Study	Virella <i>et al.</i> (2008)
1	8.39	8.38
2	3.72	3.70
3	2.80	2.78

Table 2 Convergence of total hydrodynamic pressure coefficients (C_p) for different time steps

N_t	Exciting frequency		
	28.0rad/sec	6.5rad/sec	1.5rad/sec
8	0.5876	8.7943	2.2285
16	0.6176	9.8751	2.4712
24	0.6312	9.9890	2.3937
32	0.6289	9.8753	2.4657
64	0.6289	9.8753	2.4657
128	0.6289	9.8753	2.4657

m, length of tank (L) = 0.8 m, acoustic speed (C) = 1440 m/sec, mass density of water (ρ) = 1000 kg/m³. The study is carried out against sinusoidal excitation of frequencies 28.0 rad/sec, 6.5rad/sec and 1.5 rad/sec with amplitude of 1.0g. Here, the fluid domain is discretized by 4×8 (Adhikary and Mandal 2018). Tank walls and the base are assumed to be rigid. The maximum pressure coefficient ($C_p = P / \rho * Amp * H$) for different number of time step (N_t) for different exciting frequencies are summarized in Table 2. It is observed from the tabular results that the developed hydrodynamic pressure for different exciting frequencies is converged for values of $N_t = 32$. Thus, the time step (Δt) for the analysis of water tank is adopted as $T/32$ (T =time period) for all the cases.

3.3 Analysis of liquid containers against different excitations

Here, the responses of tanks with different sizes are determined against sinusoidal excitation of different frequencies (W) such as 20%, 40%, 60%, 80%, 100% of first fundamental frequency of water within tank, second fundamental frequency of water within tank and third fundamental frequency of water within the tank. The material properties for liquid with in the tank is considered to be water and properties are follows: acoustic speed in water (C) = 1440 m/sec, mass density of water (ρ) = 1000 kg/m³. Length of tanks (L) = 20m. However, different heights (H), such as 5m ($H/L=0.25$), 10 m ($H/L=0.5$), 20m ($H/L=1.0$), 30m ($H/L=1.5$) and 40 m ($H/L=2.0$) are considered. The water is discretized by 10×10 (i.e., $N_h = 10$ and $N_v = 10$) as shown in Fig. 1. Similarly, for time history analysis the time step is considered as $T/32$.

Total hydrodynamic pressure at different levels on tank wall is plotted in Fig. 2. From Fig. 2(a) it is clear that total hydrodynamic pressure (Fig. 2i-2v) at the free surface does not depend on the height of tanks when the exciting frequency is less than the first fundamental frequency. On the other hand, the total hydrodynamic pressure (Fig. 2i(b)-2v(b)) at the mid height of wall does depend on tank height. The total hydrodynamic pressure (Fig. 2i(b)-2v(b)) decreases with the increase of tank

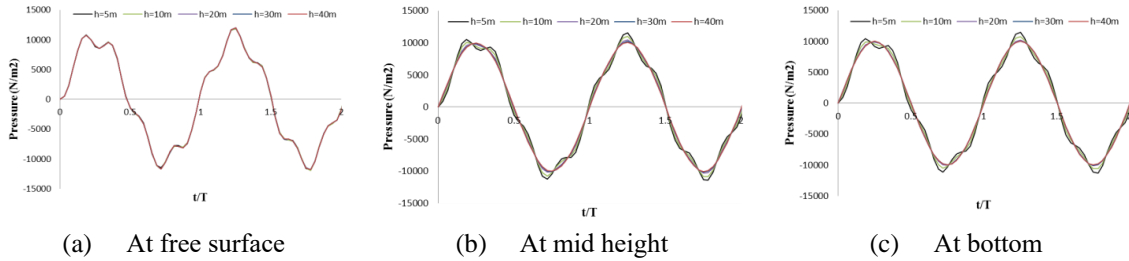


Fig. 2 Total hydrodynamic pressure for different height of tank for $W=20\%$ of first fundamental frequency

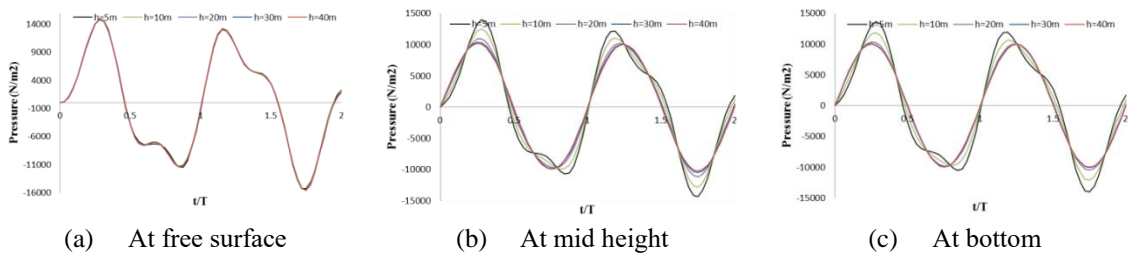


Fig. 3 Total hydrodynamic pressure for different height of tank for $W=40\%$ of first fundamental frequency

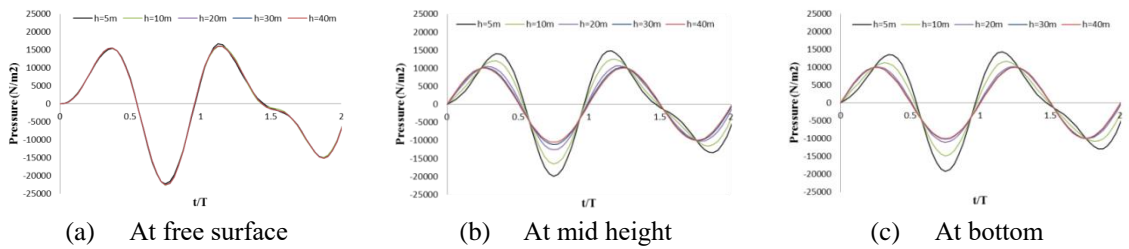


Fig. 4 Total hydrodynamic pressure for different height of tank for $W=60\%$ of first fundamental frequency

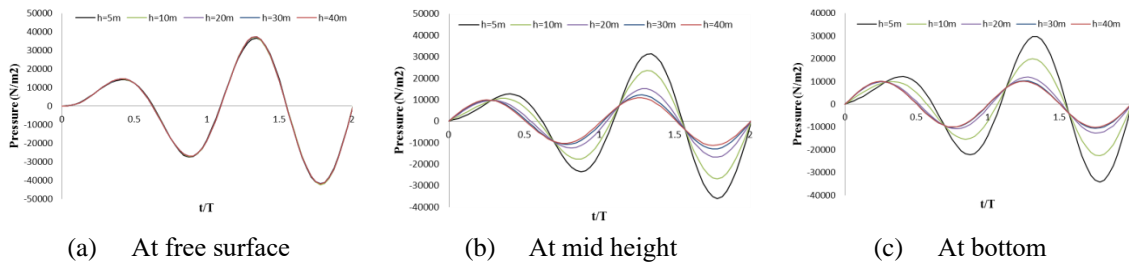


Fig. 5 Total hydrodynamic pressure for different height of tank for $W=80\%$ of first fundamental frequency

height when the exciting frequency is less than the first fundamental frequency and has a maximum value for tank height of 5 m. The trend as observed for mid height of tank is followed by the total hydrodynamic pressure (Figs. 2i(c)-2v(c)) at wall bottom. However, the total hydrodynamic pressure in all locations increases with the increase of height of tank when the exciting frequency is equal to second and third fundamental frequency of water with in the tank and it is shown in Figs. 2vi-2vii.

Total hydrodynamic pressure against different exciting frequencies is presented in Fig. 9. This

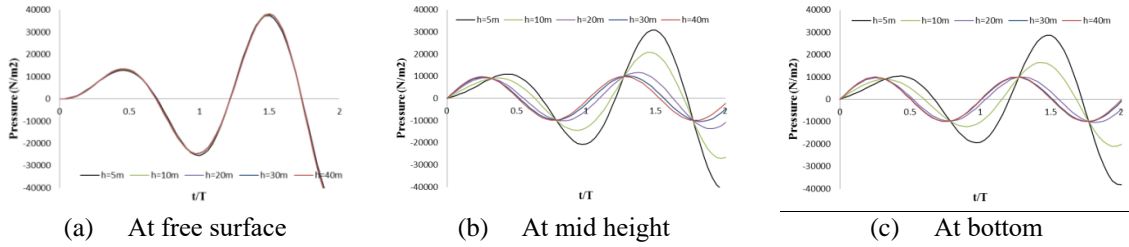


Fig. 6 Total hydrodynamic pressure for different height of tank for $W=100\%$ of first fundamental frequency

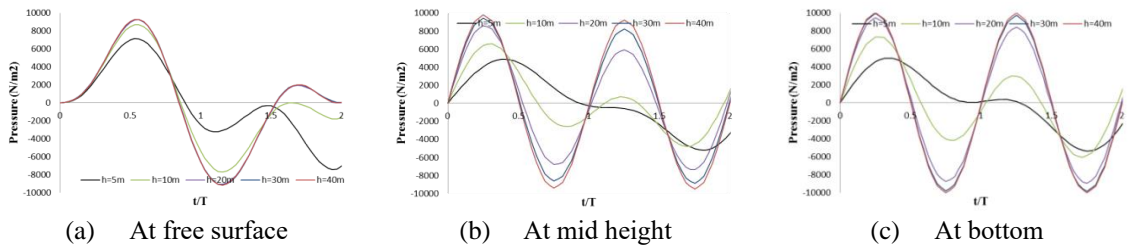


Fig. 7 Total hydrodynamic pressure for different height of tank for $W=$ Second fundamental frequency

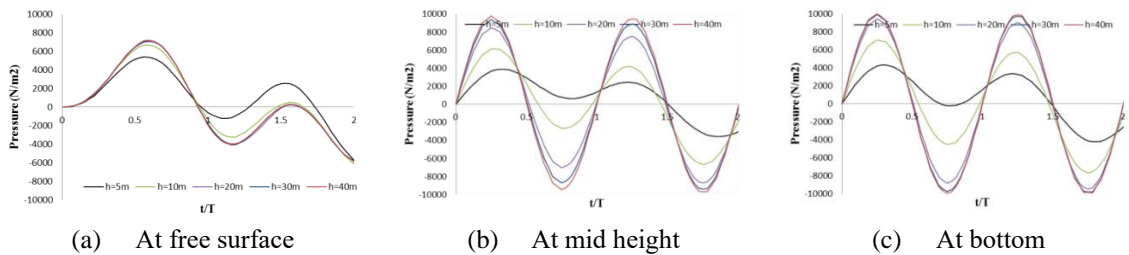


Fig. 8 Total hydrodynamic pressure for different height of tank for $W=$ Third fundamental frequency

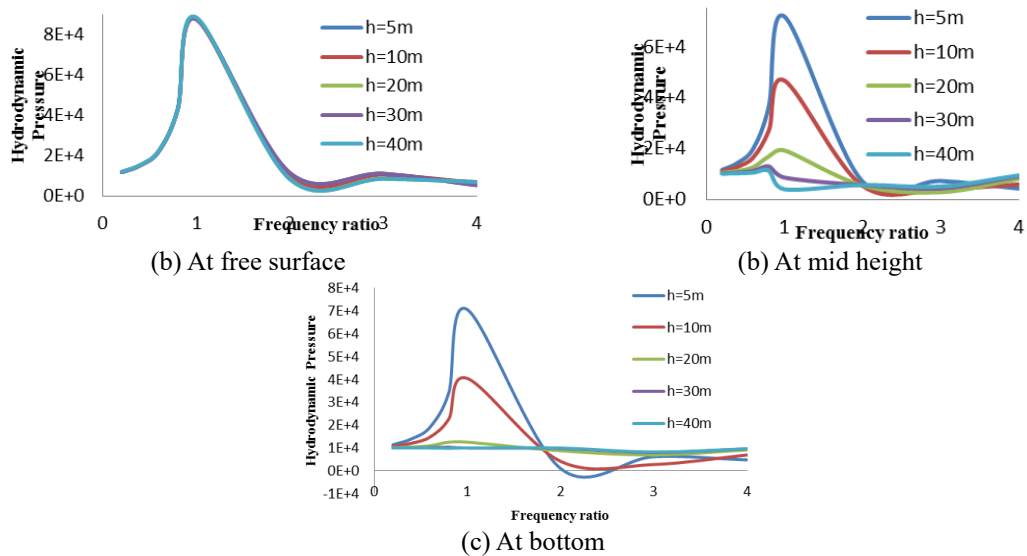


Fig. 9 Total hydrodynamic pressure for different excitation frequency

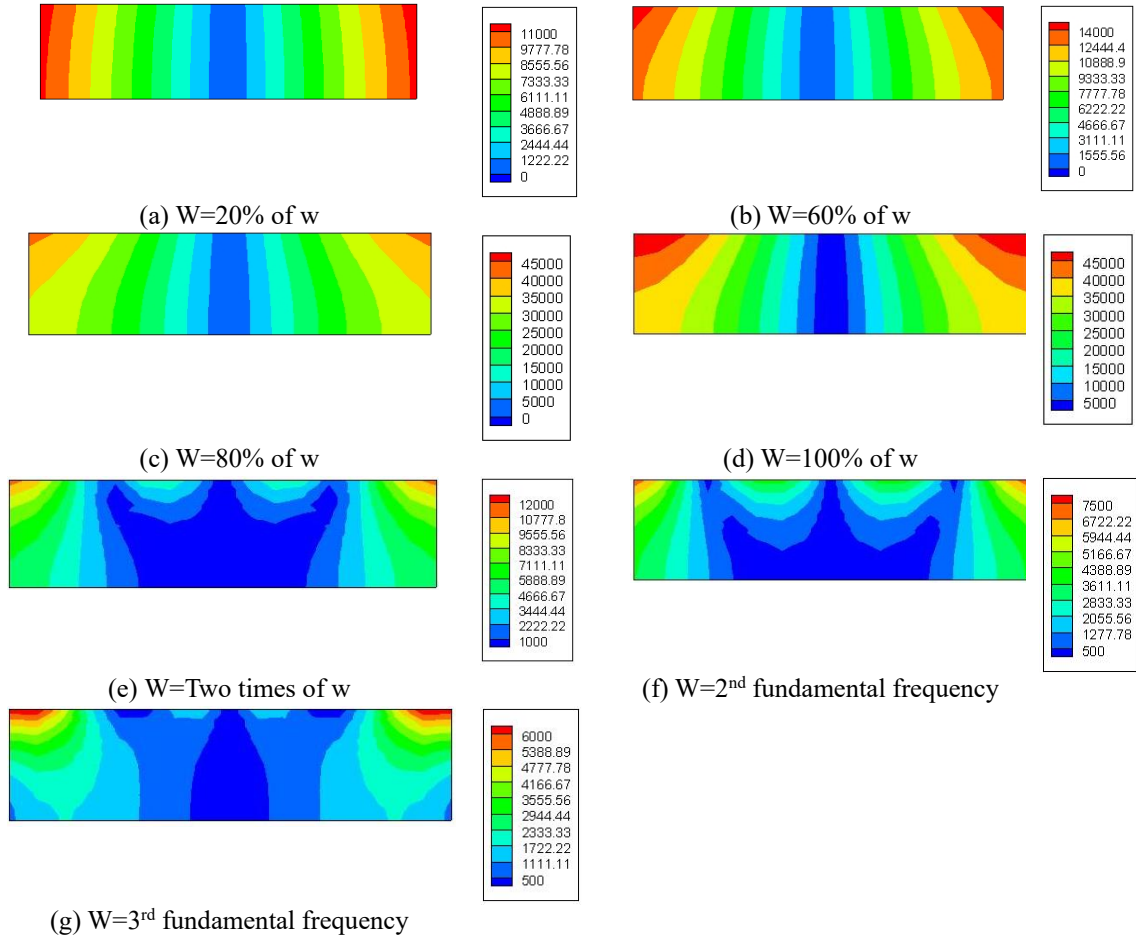


Fig. 10 Stress contour for tank of height 5 m

figure depicts that the total hydrodynamic pressure at all locations increases with the increase of exciting frequency and maximum hydrodynamic pressure occurs when the exciting frequency is equal to the fundamental frequency. After that, the hydrodynamic pressure decreases with the increase of exciting frequency. Total hydrodynamic pressure at free surface has another peak for all height of tanks when the exciting frequency is equal to three times fundamental frequency (Fig. 9(a)). However, the hydrodynamic pressure at mid height (Fig. 9(b)) and at the bottom (Fig. 9(c)) of tank wall has another peak for a particular tank height not for all heights.

Total hydrodynamic pressure contour for different height of tanks against different exciting frequencies are plotted in Figs. 10-14. Both left and right vertical walls of tank experience comparatively more hydrodynamic pressure than the other portion of the tank. However, the distribution of hydrodynamic pressure along the tank wall is different for different height of wall and exciting frequency. For comparatively lower exciting frequency, the variation of hydrodynamic pressure along the wall is not significant. However, this variation is quite significant when the exciting frequency is equal or greater than the 80% of fundamental frequency. Total hydrodynamic pressure is concentrated at two top most corners when the exciting frequency is equal to fundamental

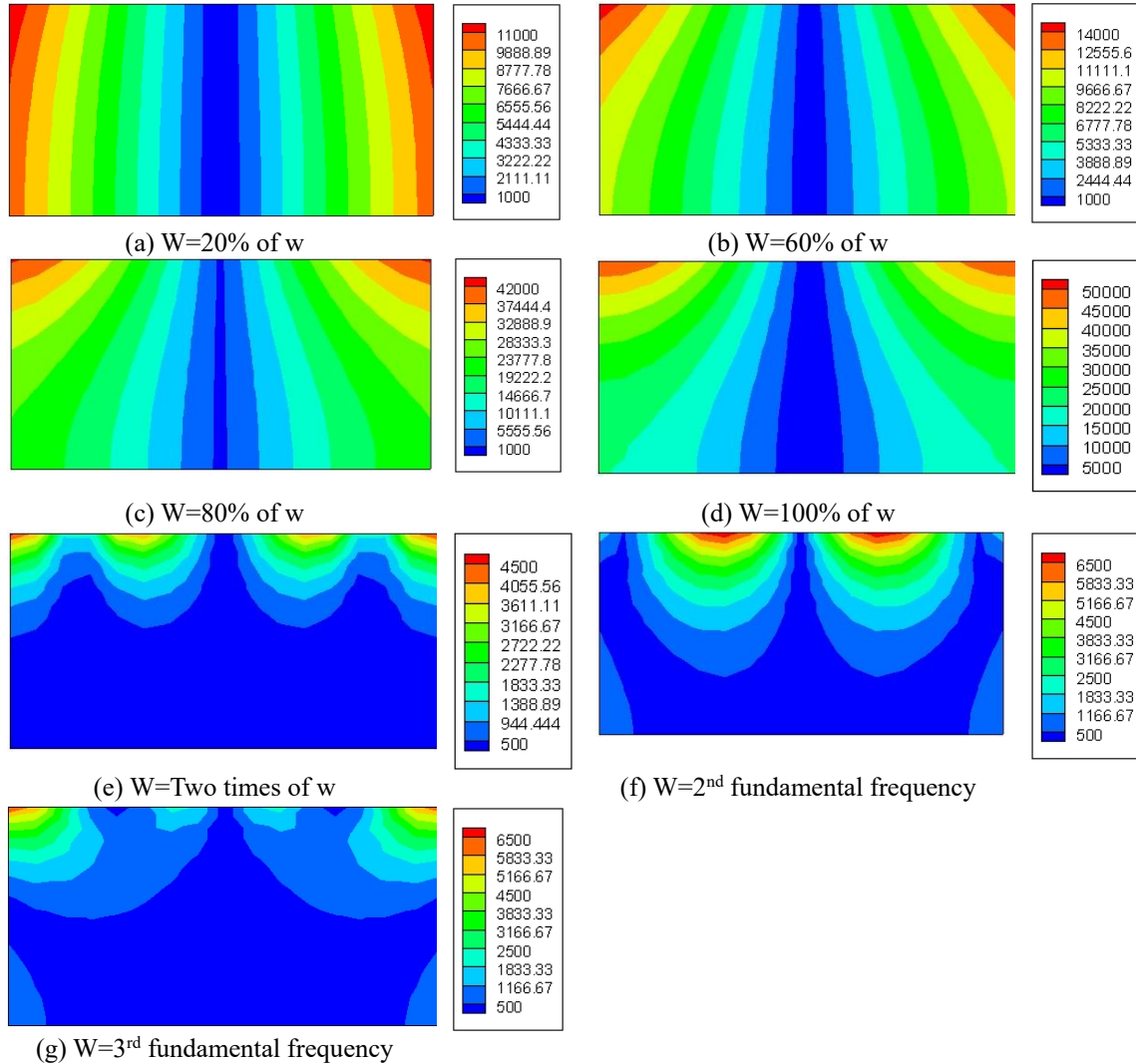


Fig. 11 Stress contour for tank of height 10 m

frequency of tank water (Figs. 10(d), 11(d), 12(d), 13(d) and 14(d)). Similarly, almost zero hydrodynamic zone near the midpoint of bottom slab of tank occurs and it is extended in upward direction with the increase of height of the tank. The total hydrodynamic pressure is concentrated at the free surface of water for comparatively lower tank height when it is excited with the frequency greater than the fundamental frequency (10e-g, 11e-g). However, the pressure not only concentrated at the free surface but also at the bottom most corners when the height of tanks is greater than 10 m (12e-g, 13e-g, 14e-g).

Vertical displacements along the free surface of water are also plotted for different exciting frequencies in Fig. 15. From this figure it is clear that the sloshing does not depend on height of tanks. However, it is dependent on the exciting frequency. The sloshed displacement increases with the increase of exciting frequency and has maximum value when it is excited with fundamental

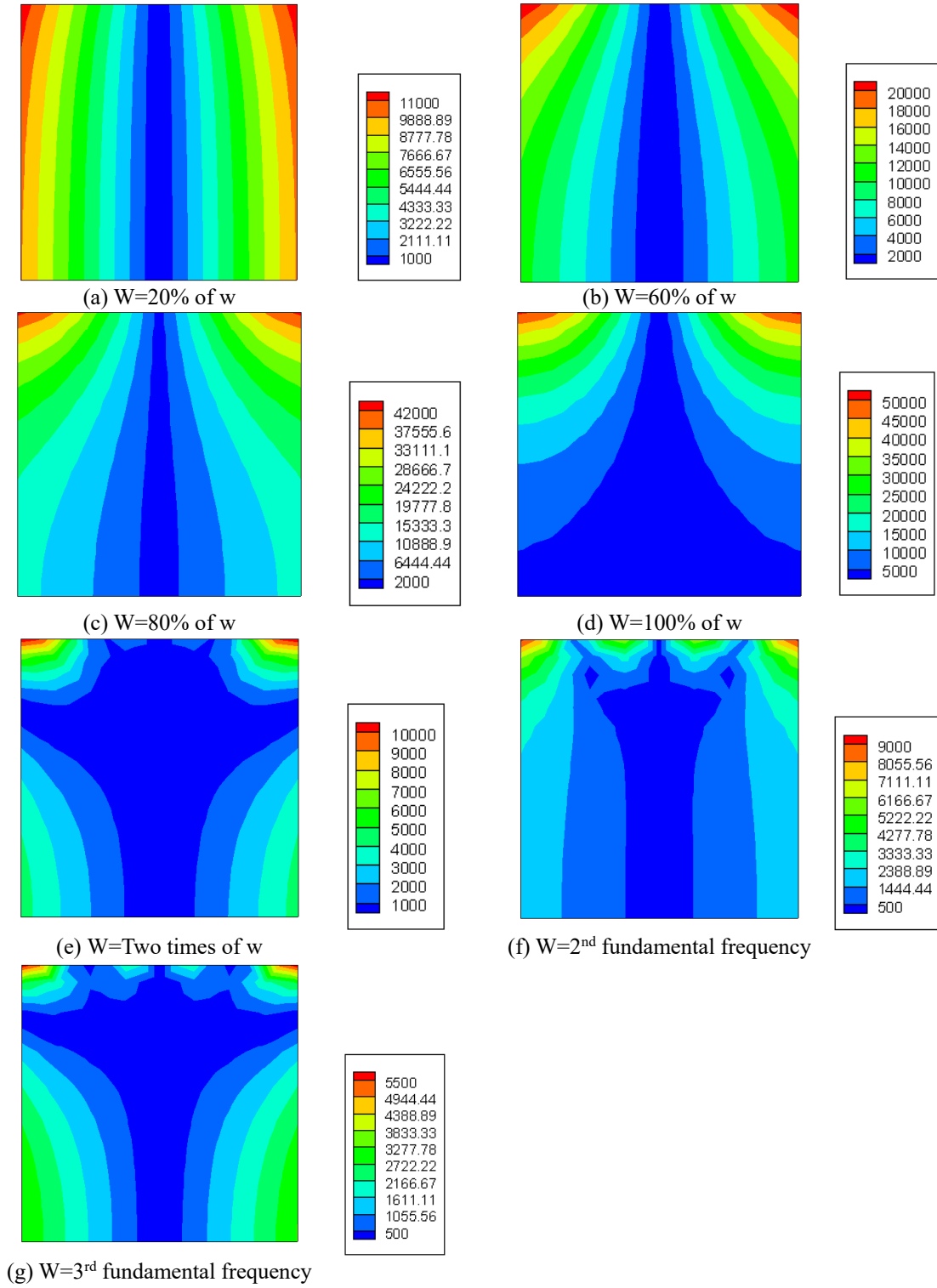


Fig. 12 Stress contour for tank of height 20 m

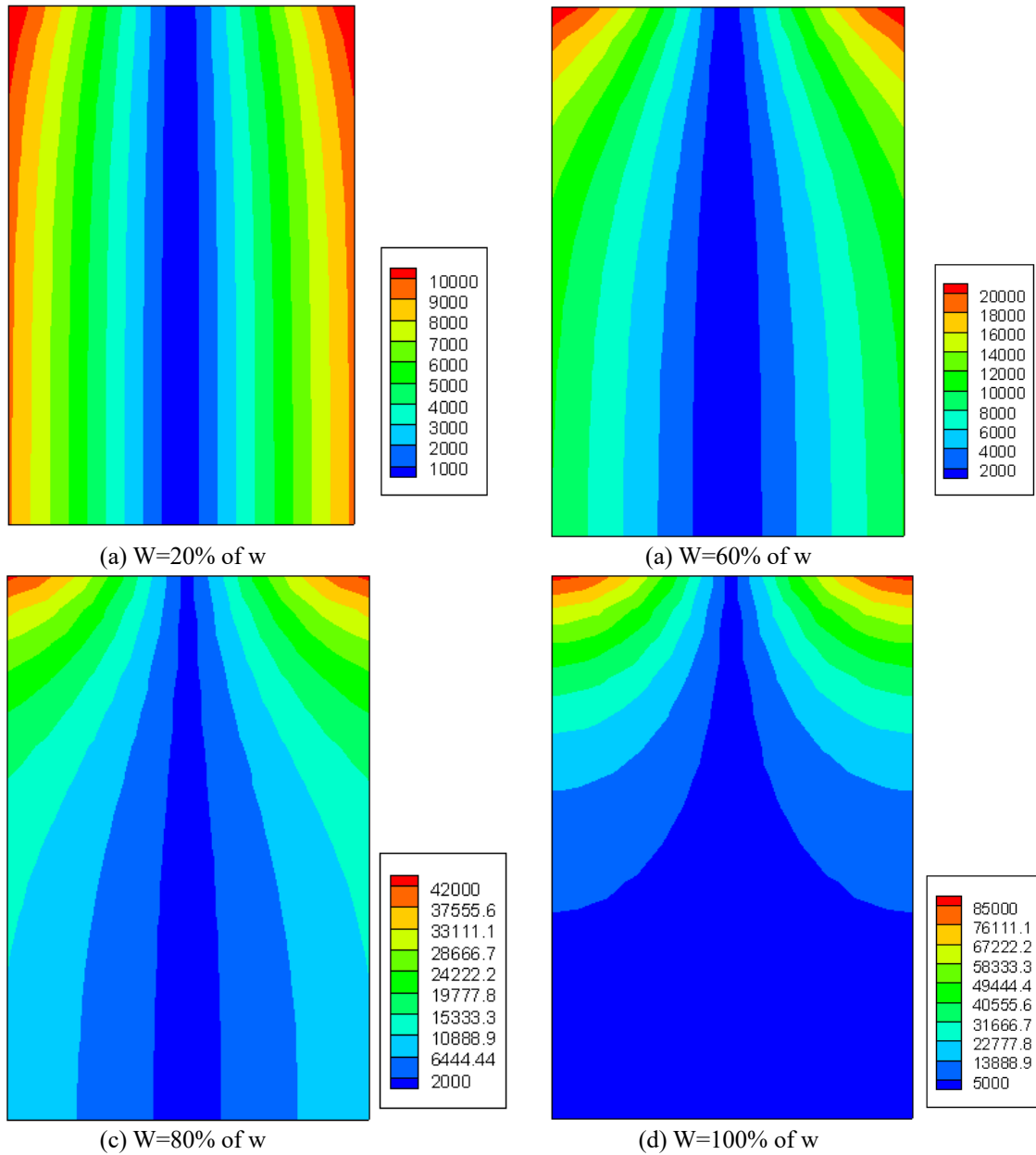


Fig. 13 Stress contour for tank of height 30 m

frequency. However, the sloshing is quite less when the exciting frequency is greater than the fundamental frequency of water within the tank. It is also interesting to see that the sloshed displacement for a particular exciting frequency does not depend on the tank height.

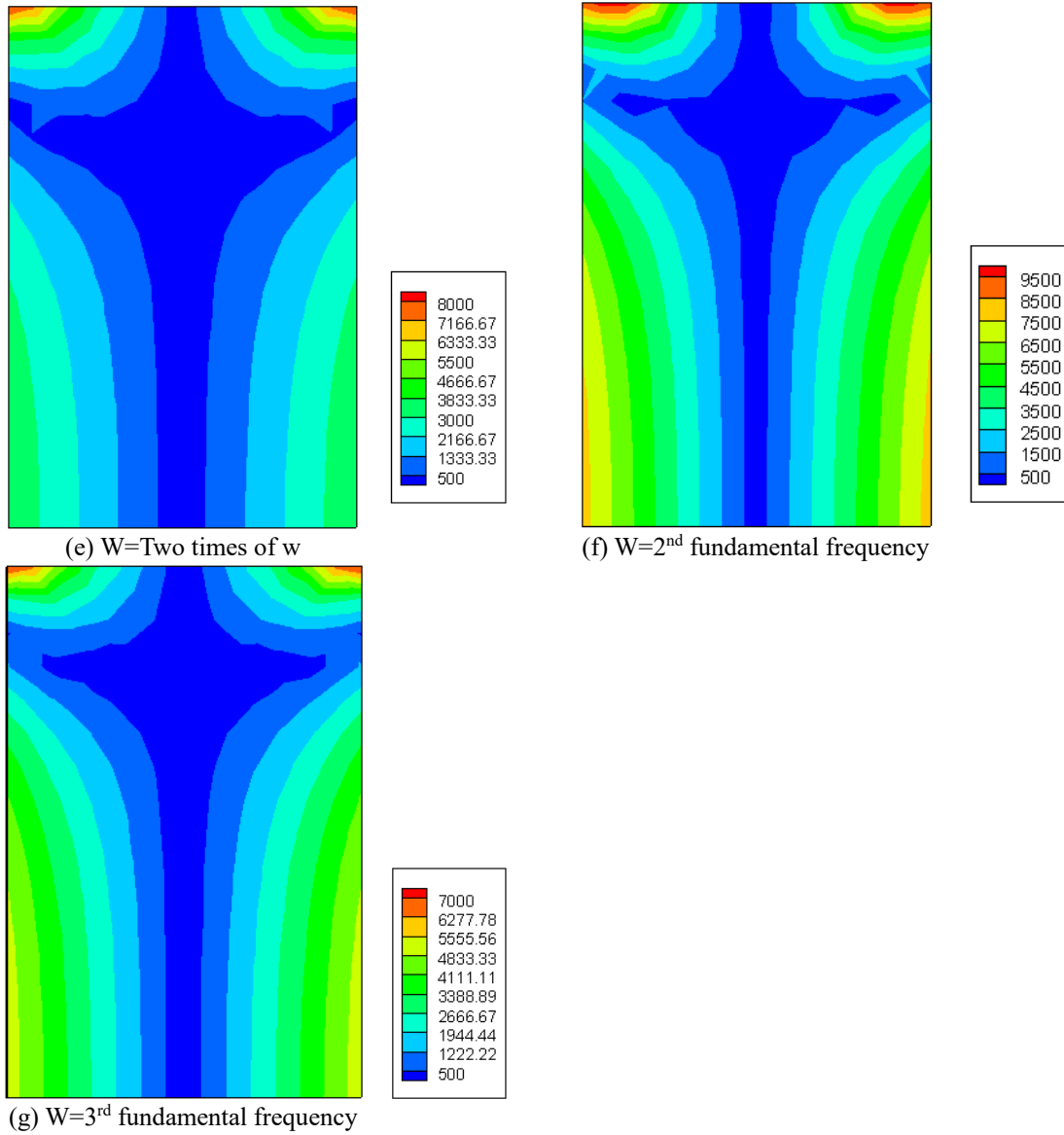


Fig. 13 Continued-

4. Conclusions

The behavior of total hydrodynamic pressures of rectangular water tank against different exciting frequencies is studied. The liquid within the tank is considered to be linearly compressible. A pressure based finite element method is used to simulate the liquid in the tank and walls of tank are considered to be rigid.

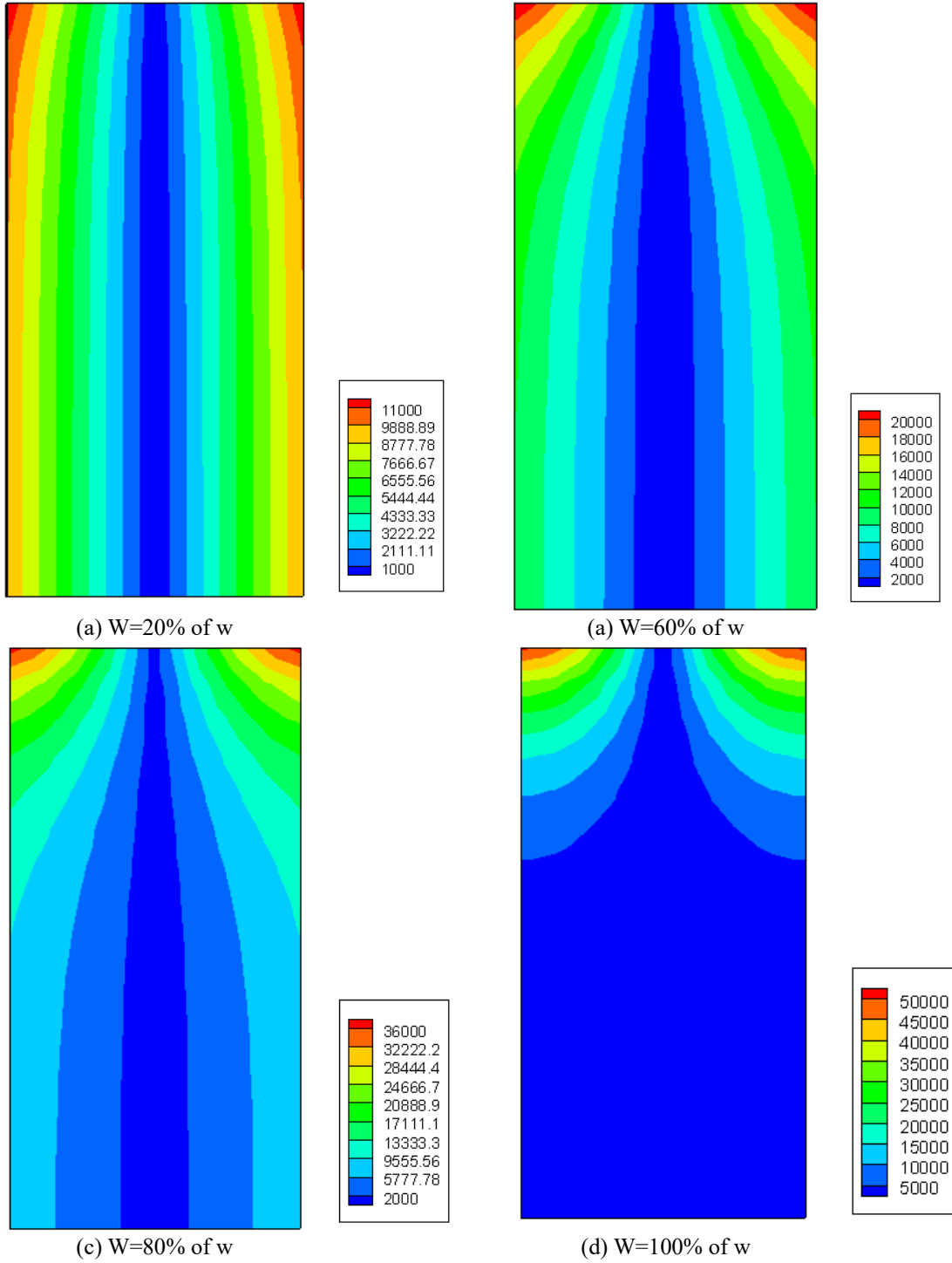
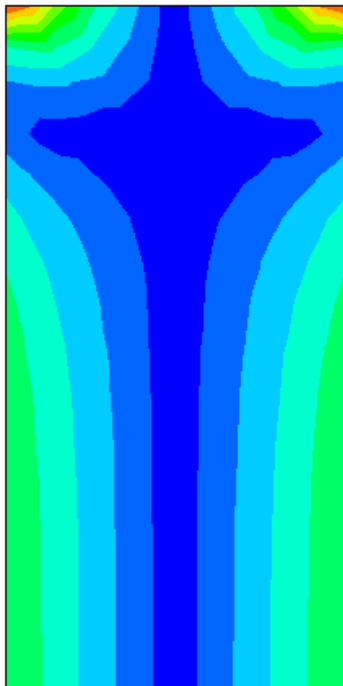
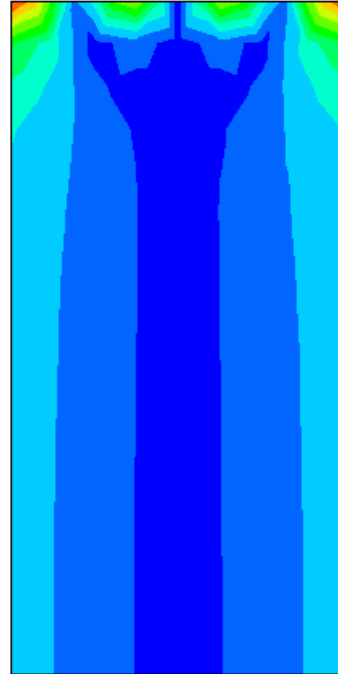


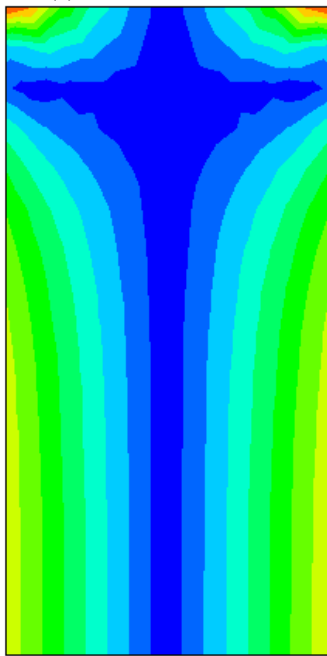
Fig. 14 Stress contour for tank of height 40 m



(e) $W=2$ times of w



(f) $W=2^{\text{nd}}$ fundamental frequency



(g) $W=3^{\text{rd}}$ fundamental frequency

Fig. 14 Continued-

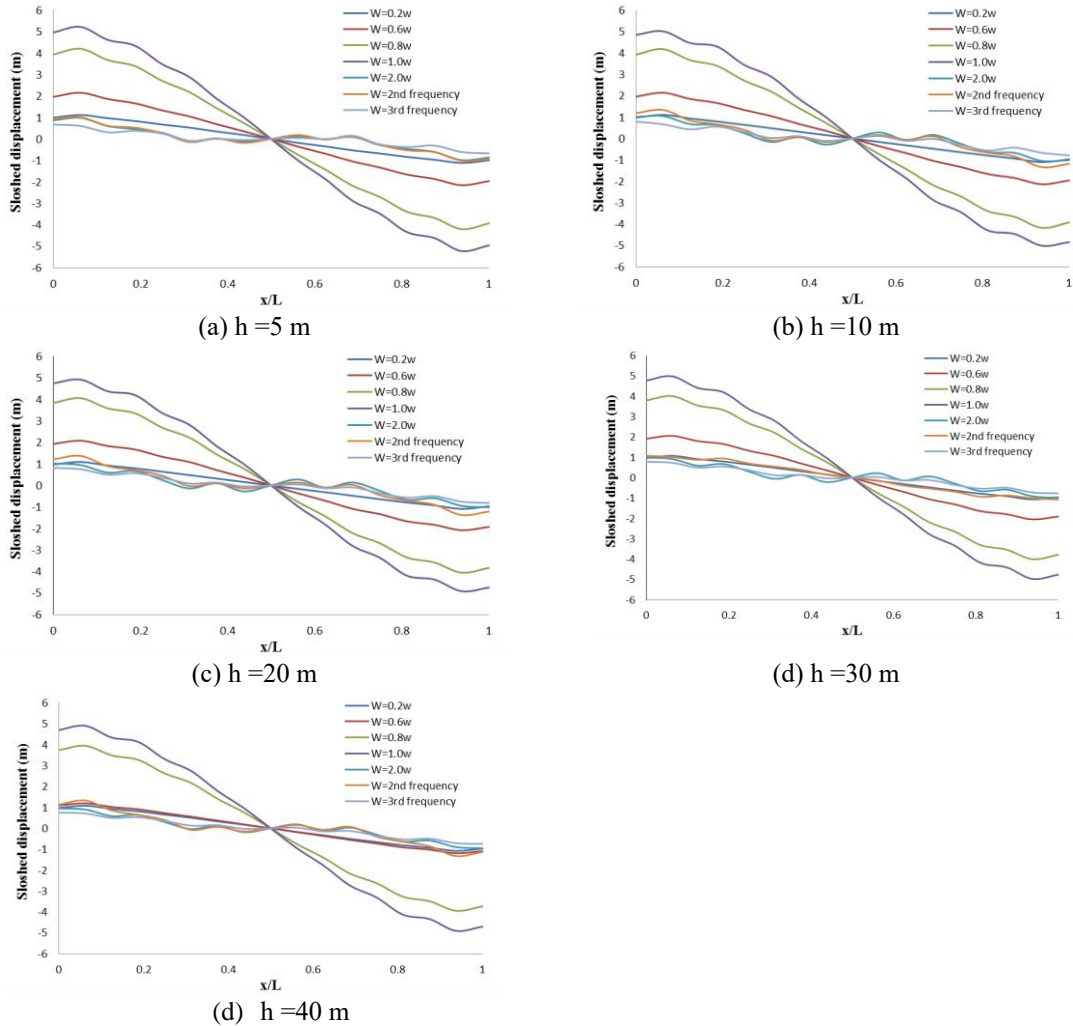


Fig. 15 Sloshed displacements of tanks

The total hydrodynamic pressure and displacement at the free surface of liquid are considered to be the main aspect during design of such tanks. In the present study, the total hydrodynamic pressure on vertical walls of different sizes against different exciting frequencies is determined as the total hydrodynamic pressure is considered to be the major disturbing force on the tank during seismic excitation. The total hydrodynamic pressure within tank depends on exciting frequencies as well as the height of rectangular water tank. Total hydrodynamic pressure increases with the increases of exciting frequency when the exciting frequency is less than the fundamental frequency of the liquid within the tank and it has maximum value for exciting frequency is equal to fundamental frequency. The total hydrodynamic pressure has decreasing trend for exciting frequency greater than the fundamental frequency of liquid. For a particular exciting frequency, the total hydrodynamic pressure at the free surface of liquid is independent of tank length. However, the hydrodynamic

pressure at base and mid height of vertical wall decreases with the increase of height of liquid within tank. The distribution of hydrodynamic pressure within liquid domain changes continuously with the change of exciting frequency. This distribution is smooth when the exciting frequency is less than the fundamental frequency. The depth of undisturbed zone of liquid increases with the increase of liquid height when the exciting frequency is equal to the fundamental frequency of liquid.

The vertical displacement at free surface does not depend on height of tanks. However, it depends on exciting frequency. The sloshed displacement increases with the increase of exciting frequency and has maximum value when the exciting frequency is equal to the fundamental frequency of liquid within the tank. However, the sloshing is quite less when the exciting frequency is greater than the fundamental frequency. In practice, this free surface elevation during dynamic excitation is required to provide the free board within the tanks.

References

- Adhikary, R. and Mandal, K.K. (2018), "Dynamic analysis of water storage tank with rigid block at bottom", *Ocean Syst. Eng.*, **8**(1), 57-77. <https://doi.org/10.12989/ose.2018.8.1.057>.
- Ali, A.Q. and Telang, D.P. (2017), "A survey on dynamic analysis of elevated water tank for different staging configuration", *J. Computer Sci. Mobile Com.*, **6**(5), 194-201.
- Algreane, G.A.I., Osman, S.A., Karim, O.A. and Kasa, A. (2011), "Study the fluid structure interaction due to dynamic response of elevated concrete water tank", *Aust. J. Basic Appl. Sci.*, **5**(9), 1084-1087.
- Arafa, M. (2007), "Finite element analysis of sloshing in rectangular liquid-filled tanks", *J. Vib. Control*, **13**(7), 883-903. <https://doi.org/10.1177/1077546307078833>.
- Aregawi, B. and Kassahun, A. (2017), "Dynamic Response of ground supported rectangular water tanks to earthquake excitation", *Momona Ethiopian J. Sci.*, **9**(1), 66-75. <https://doi.org/10.4314/mejs.v9i1.5>.
- .Avval, I.T. (2012), "Dynamic response of concrete rectangular liquid tanks in three-dimensional space", *Theses and dissertations*. <http://digitalcommons.ryerson.ca/dissertations>.
- Bhojavia, R. and Dhyani, D.J. (2018), "Comparative seismic analysis of ground supported circular water tank using codal provision", *Proceedings of the 2nd Inter. Conf. of Current Research Trends in Engg. and Technology*, **4**(5), 2394-4099.
- Bouaanani, N., Goulmot, D. and Miquel, B. (2012), "Seismic response of asymmetric rectangular liquid-containing structures", *J. Eng. Mech.*, **138**(10), 1288-1297. [https://doi.org/10.1061/\(ASCE\)EM.1943-7889.0000423](https://doi.org/10.1061/(ASCE)EM.1943-7889.0000423).
- Chen, J.Z. and Kianoush, M.R. (2004), "Response of concrete liquid containing structures in different seismic zones", *Proceedings of the 13th World Conf. on Earthquake Eng.*, Paper No. 1441.
- Chu, R.C., Wu, R.Y., Wu, R.T. and Wang, C.Y. (2018), "Slosh-induced hydrodynamic force in a water tank with multiple baffles", *Ocean Eng.*, **167**, 282-292. <https://doi.org/10.1016/j.oceaneng.2018.08.049>.
- Dudhatra, K. and Desani, V. (2016), "Parametric study of hydrodynamic pressure for ground rested rectangular RC tank", *Int. J. Sci. Develop. Res.*, **1**(5), 259-264.
- Gill, S. (1951), "A process for the step-by-step integration of differential equations in an automatic digital computing machine", *Proceedings of the Cambridge Philosophical Society*, **47**, 96-108.
- Hejazi, F.S.A. and Mohammadi, M.K. (2019), "Investigation on sloshing response of water rectangular tanks under horizontal and vertical near fault seismic excitations", *J. Soil Dynam. Earthq. Eng.*, **116**, 637-653. <https://doi.org/10.1016/j.soildyn.2018.10.015>.
- Hemalatha, P. and Rao, K.V.M. (2018), "Analytical interpretation of hydrodynamic pressure causing slosh effect on overhead water tank", *Int. J. Recent Res. Aspects*, **5**(1), 328-332.
- Jena, D. and Biswal, K.C. (2017), "A numerical study of violent sloshing problems with modified MPS method", *J. Hydrodynam.*, **29**(4), 659-667. [https://doi.org/10.1016/S1001-6058\(16\)60779-5](https://doi.org/10.1016/S1001-6058(16)60779-5).
- Kang, H.S., Arif, U.G., Kim, K.S., Kim, H.M., Liu, Y.J., Lee, K.Q. and Wu, Y.T. (2019), "Sloshing suppression

- by floating baffle”, *Ocean Syst. Eng.*, **9**(4),409-422. <https://doi.org/10.12989/ose.2019.9.4.409>.
- Kolai, A. and Rakheja, S. (2018), “Free vibration analysis of coupled sloshing-flexible membrane system in a liquid container”, *J. Vib. Control*, **25**(1), 84-97.
- Kotrasova, K. (2017), “Influence of horizontal seismic excitation on tank-fluid-soil interaction”, *Civil Eng. Series*, **17**(1), 45-56.
- Kotrasova, K. and Kormanikova, E. (2018), “Frequency analysis of partially-filled rectangular water tank”, *Int. J. Mech.*, **12**, 59-66.
- Mandal, K.K. and Maity, D. (2016), “Nonlinear finite element analysis of water in rectangular tank”, *Ocean Eng.*, **121**, 592-601. <https://doi.org/10.1016/j.oceaneng.2016.05.048>.
- Ming, P.J. and Duan, W.Y. (2010), “The numerical simulation of sloshing in rectangular tank with VOF based on unstructured grids”, *J. Hydrodynam.*, **22**(6), 856-864. [https://doi.org/10.1016/S1001-6058\(09\)60126-8](https://doi.org/10.1016/S1001-6058(09)60126-8).
- Mingzhen, W. and Lin, G. (2018), “Dynamic time-history analyses of ground reinforced concrete tank in water supply system under bi-directional horizontal seismic actions”, *Adv. Eng. Res.*, **163**, 123-135.
- Nguyen, H.X., Dinh, V.N. and Basu, B. (2021), “A comparison of smoothed particle hydrodynamics simulation with exact results from a nonlinear water wave model”, *Ocean Syst. Eng.*, **11**(2),185-201. <https://doi.org/10.12989/ose.2021.11.2.185>.
- Pajand, M.R. (2016), “Analytical solution for free vibration of flexible 2D rectangular tanks”, *Ocean Eng.*, **122**, 118-135. <https://doi.org/10.1016/j.oceaneng.2016.05.052>.
- Patel, C.H., Vaghela, S.N. and Patel, H.S. (2012), “Sloshing response of elevated water tank over alternate column proportionality”, *Int. J. Adv. Eng. Technol.*, **3**(4), 60-63.
- Ralston, A. and Wilf, H.S. (1965), *Mathematical Models for Digital Computers*, Wiley, New York.
- Rawat, A., Mittal, V., Chakraborty, T. and Matsagar, V. (2019), “Earthquake induced sloshing and hydrodynamic pressures in rigid liquid storage tanks analyzed by coupled acoustic-structural and Euler-Lagrange methods”, *Thin-Wall. Struct.*, **134**, 333-346. <https://doi.org/10.1016/j.tws.2018.10.016>.
- Saghi, H. (2016), “The pressure distribution on the rectangular and trapezoidal storage tanks' perimeters due to liquid sloshing phenomenon”, *Int. J. Naval Architect. Ocean Eng.*, **8**(2), 153-168. <https://doi.org/10.1016/j.ijnaoe.2015.12.001>.
- Sahaj, K.V., Nasar, T. and Vijay, K.G. (2021), “Experimental study on liquid sloshing with dual vertical porous baffles in a sway excited tank”, *Ocean Syst. Eng.*, **11**(4), 535-371. <https://doi.org/10.12989/ose.2021.11.4.353>.
- Sanapala, V.S., Sajisha, S.D., Velusamy, K., Ravisankara, A. and Patnaik, B.S.V. (2019), “An experimental investigation on the dynamics of liquid sloshing in a rectangular tank and its interaction with an internal vertical pole”, *J. Sound Vib.*, **449**, 43-63. <https://doi.org/10.1016/j.jsv.2019.02.025>.
- Shekari, M.R., Hekmatzadeh, A.A. and Amiri, S.M. (2019), “On the nonlinear dynamic analysis of base-isolated three-dimensional rectangular thin-walled steel tanks equipped with vertical baffle”, *Thin-Wall. Struct.*, **138**, 79-94. <https://doi.org/10.1016/j.tws.2019.01.037>.
- Virella, J.C., Prato, C.A. and Godoy, L.A. (2008), “Linear and nonlinear 2D finite element analysis of sloshing modes and pressures in rectangular tanks subject to horizontal harmonic motions”, *J. Sound Vib.*, **312**(3), 442-460. <https://doi.org/10.1016/j.jsv.2007.07.088>.
- Wakchaure, M.R. and Besekar, S.S. (2014), “Behaviour of elevated water tank under sloshing effect”, *Int. J. Eng. Res. Technol.*, **3**(2), 2278-0181.
- Yazdaniyan, M., Razavi, S.V. and Mashal, M. (2016), “Seismic analysis of rectangular concrete tanks by considering fluid and tank interaction”, *J. Solid Mech.*, **8**(2), 435-445.
- Yazdabad, M., Behnamfar, F. and Samani, A.K. (2018), “Seismic behavioral fragility curves of concrete cylindrical water tanks for sloshing, cracking, and wall bending”, *Earthq. Struct.*, **14**(2), 95-102. <https://doi.org/10.12989/eas.2018.14.2.095>.
- Zhao, M. and Zhou, J. (2018), “Review of seismic studies of liquid storage tanks”, *Struct. Eng. Mech.*, **65**(5), 557-572. <https://doi.org/10.12989/sem.2018.65.5.557>.
- Zhao, D., Hub. Z., Chen, D., Limb. S. and Wange, S. (2018), “Nonlinear sloshing in rectangular tanks under forced excitation”, *Int. J. Naval Architect. Ocean Eng.*, **10**(5), 545-565. <https://doi.org/10.1016/j.ijnaoe.2017.10.005>.

Zhong, L. (2018), "Seismic design and analysis of concrete liquid-containing tanks", *Structures Congress* 2018, 444-454.

RS